Geothermics 125 (2025) 103152

Contents lists available at ScienceDirect

Geothermics

journal homepage: www.elsevier.com/locate/geothermics

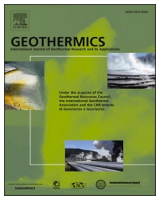

Uni-directional ATES in high groundwater flow aquifers

Valerio Silvestri [a,*], Giovanni Crosta [a], Alberto Previati [a], Paolo Frattini [a], Martin Bloemendal [b,c]

[a] University of Milano Bicocca, Department of Earth and Environmental Sciences, Milan, Italy
[b] Delft University of Technology, Faculty of Civil Engineering and Geosciences, Delft, Netherlands
[c] TNO, Dutch Geological Survey, Utrecht, Netherlands

ARTICLE INFO

Keywords:
Aquifer thermal energy storage
Groundwater heat pump
Groundwater flow velocity
Inter-well distance
Thermal recovery efficiency
Thermal plume

ABSTRACT

Aquifer thermal energy storage (ATES) is attained by storing thermal energy in aquifers, using the groundwater as a carrier for the heat. Hence, in ATES systems, the background groundwater flow velocity may affect the efficiency if a significant amount of stored heat is moved away from the storage well by advection. This paper presents an alternative solution to the typical "pump and dump" open-loop shallow geothermal system configuration using the ATES concept with a reversed extraction-injection well scheme. This particular placement is able to increase the energy efficiency of a conventional open-loop system while reducing the thermal impact downstream the system.

The uni-directional ATES pumping scheme compensates the heat transport by groundwater flow extracting the groundwater from the downstream well and re-injecting back in the upstream well. This research presents a numerical feasibility study and sensitivity analysis of the effects of the well spacing, pumping scheme and groundwater flow velocity on the efficiency of a uni-directional ATES. Optimal combinations are suggested to ensure the maximum re-capture by the downstream well of the heat injected in the upstream well in the previous season and subject to thermal transport by advection, with a maximum heat recovery between 55 and 75 % depending on the conditions. The results of the modelling analysis showed that the optimal inter-well distance depends on the groundwater flow velocity and the total annual storage volume. This paper also demonstrates the mitigation effect of the thermal perturbation downstream of a uni-directional ATES compared to a conventional open-loop scheme.

1. Introduction

The European plan proposed in July 2021 in the context of the European Green Deal (Fit for 55), requires all member states to reduce their greenhouse gas (GHG) emissions by 55 % before 2030, as an intermediate step towards the net zero goal by 2050 aiming to limit the global warming to 1.5 °C compared to pre-industrial levels (European Council, 2021). Hence, cities all over Europe are adopting sustainable energy systems to reach this objective. Heating and cooling of buildings account for 54 % of the total GHG emissions in Italy in 2018 (ISPRA, 2020), in Europe decreases to 36 % (European Council, 2021), and across the world, it contributes to about 40 % of all primary energy use (IRENA, 2023). Ground source heat pumps are a renewable solution that many countries are adopting to replace fossil-based heating and cooling techniques (Banks, 2009). Such systems use the ground and/or groundwater to reject, extract, and/or store heat in the underground. When groundwater (GW) in aquifers is used for the storage of heat, such system is called aquifer thermal energy storage (ATES). This system consists of one or more pairs of wells (a doublet), which have a bi-directional flow scheme: from warm to cold well in winter and from cold to warm in the summer. As aquifers are commonly present in urban areas, these systems have great potential for decarbonizing the heating and cooling supply of buildings (Bloemendal et al., 2015).

ATES technology is known to reduce significantly CO_2 emissions for heating and cooling buildings (Fleuchaus et al., 2020). In this document two types of ATES systems are investigated considering variable GW flow velocity. Several previous studies have been conducted to explore the feasibility of ATES systems in high GW velocity by numerical modelling (Lee, 2014; Bloemendal and Olsthoorn, 2018; Stemmle et al. 2023). Generally, conventional open-loop (O-L) systems (Fig. 1c) are the most used configuration, independently to the GW flow velocity. These systems extract the GW from an upstream well and re-inject it in a downstream well in both seasons. In this last case, the efficiency of the system is lower, due to the smaller energy content of the GW.

* Corresponding author.
E-mail address: v.silvestri12@campus.unimib.it (V. Silvestri).

https://doi.org/10.1016/j.geothermics.2024.103152
Received 5 March 2024; Received in revised form 1 August 2024; Accepted 27 August 2024
Available online 5 September 2024

Furthermore, such systems generate thermal plumes that affect the downstream GW temperature.

Previous studies (Bloemendal and Olsthoorn, 2018), demonstrated for low GW flow velocity contexts (less than 25 m/year) the high efficiency of an ATES configuration (Fig. 1a) with respect to an O-L operation scheme, taking the advantage of storing and re-using the wasted heat/cold in the previous season.

Alternatively, with multiple doublets systems special design is needed to limit the advection losses of the stored warm and cold GW caused by its flow. Such designs require either, multiple doublets (Fig. 1b) in which the water is pumped from the downstream well in one season and injected in the upstream in the other, as proposed by Bloemendal & Olsthoorn (2018). However, these systems require at least two well doublets, and a specific placement distance, which may be difficult to achieve in an urban setting.

To benefit from groundwater heat storage where ambient GW flow is high, a combination of the two solutions described above is proposed by applying a uni-directional pumping scheme (Fig. 1d). In this configuration, the GW is extracted from a downstream well and re-injected into an upstream well. Proper spacing of the wells allows re-capturing of the energy stored in the aquifer in the upstream well, which is transported to the downstream extraction well by the natural GW flow. Optimal

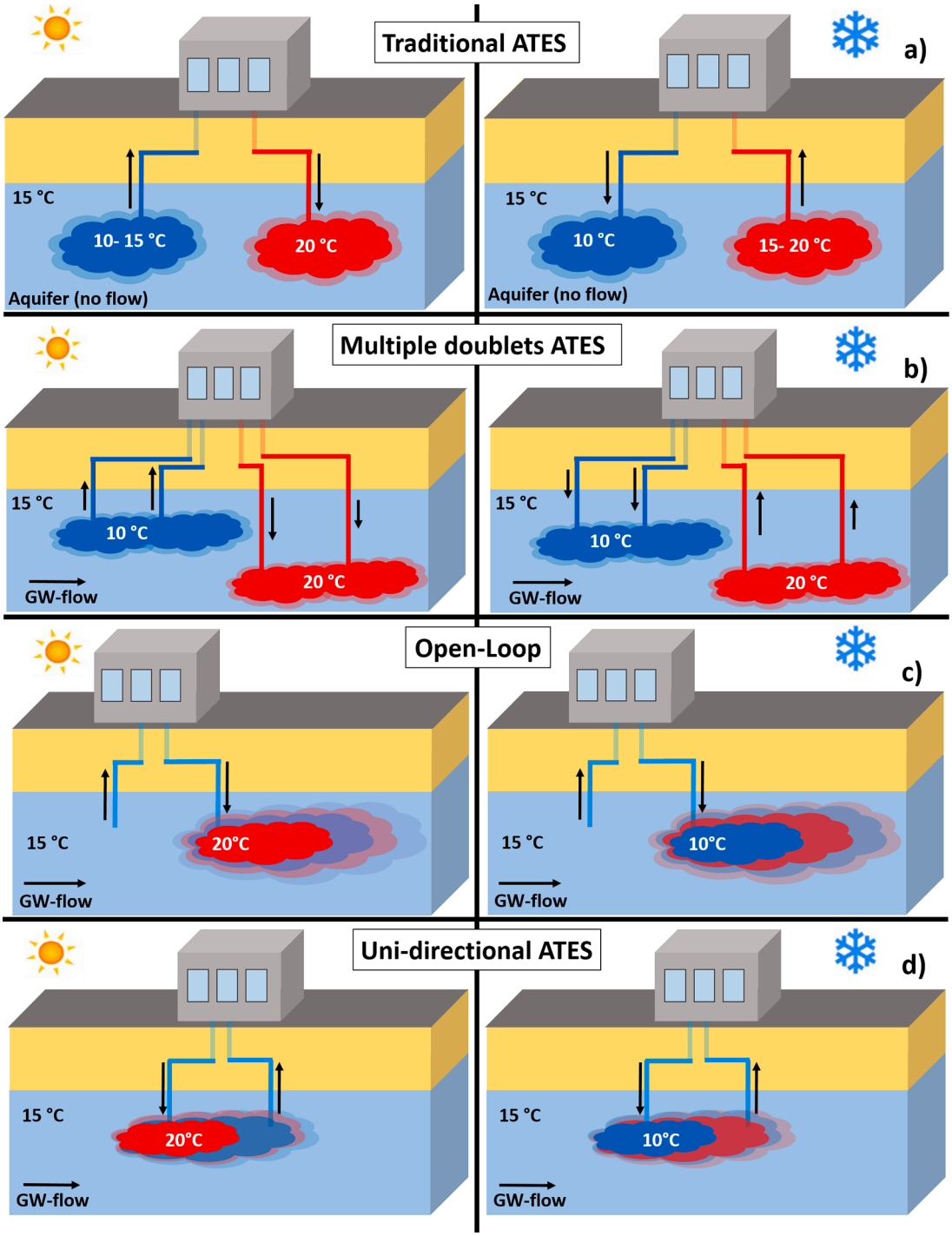

Fig. 1. Schematic representation of: a) traditional ATES (Bloemendal et al., 2018) b) multiple doublets, (Bloemendal and Olsthoorn, 2018; Stemmle et al. 2023,), c) conventional open loop, d) uni-directional ATES. (Double column 16 cm width).

placement of the wells will depend on GW flow velocity and the total volume stored in summer and winter. This configuration can also mitigate the intensity of the downstream thermal perturbation. The design considerations and how to space such wells are yet to be defined.

Hence, the goal of this paper is to assess and quantify under which conditions a uni-directional ATES (UD-ATES) well design and pumping scheme is a feasible concept for storying the energy in aquifers with a high GW flow velocity. It is also determined the optimal inter-well distance for each seasonal storage and groundwater flow conditions.

2. Methods

A sensitivity analysis based on a hydrothermal dynamic model is proposed to assess the feasibility by varying a wide range of relevant geothermal systems and aquifer characteristics.

2.1. MODFLOW/MT3DMS and model description

To take into consideration all the physical properties governing the GW heat flow, such as thermal conduction and advection, flopy package (Bakker et al., 2016) for running MODFLOW (Harbaugh et al., 2000) MT3DMS transport code (Zheng and Wang, 1999) have been used. This 3D Finite Difference numerical Model (FDM) solves the GW flow and heat transport equations, allowing the simulation of the extraction and injection of the GW from wells, the hydrodynamic regime, and the thermal transport, like in other previous studies conducted on ATES systems (Bloemendal and Hartog, 2018; Rostampour et al., 2019; Bloemendal and Olsthoorn, 2018).

2.1.1. Synthetic model description and validation

A synthetic box model was generated with the following characteristics:

- Model layers: the thickness of the main aquifer is 20 m (horizontal hydraulic conductivity [Kh] is 10 m/d), and it is confined by two clay horizons (Kh = 0.05 m/d) with the same thickness. The vertical hydraulic conductivity is considered to be 1/5 of the horizontal hydraulic conductivity and the porosity for all the layers is 0.3. Each layer is divided in four simulation layers, obtaining 12 slices of 5 m for the whole vertical discretization of the model (Fig. 2a).
- Boundary conditions: the model boundaries are constant head and temperature of 15 °C. The head boundaries are varied during the sensitivity analysis chosen such that the gradient together with the hydraulic conductivity result in different groundwater flow velocities, ranging from 3 m/y up to 1000 m/y. Fluid sink and source terms are applied at well locations (extraction and injection well, respectively) to simulate the operative configuration of the system. An additional temperature differential is applied to the reinjected water to the temperature of the extracted water using a Dirichlet type boundary condition.
- Spatial discretization: the horizontal grid is 10 × 10 m in size around the wells, gradually increasing up to 100 × 100 m at the edges of the model (Fig. 2b). The element size of the central part of the grid was chosen to obtain a good accuracy minimizing the computation time for model. This parameter was evaluated for squares of 3, 5, 10, 20, 50 and 70 m displaying an incremental error according to the efficiency outcome (the baseline considered is for 3 × 3 m square grid). With a grid of 10 × 10 m the error is kept below 5 % and only with cells greater than 20 × 20 the error increases up to 10 %.
- Temporal discretization: a seven-day time step was chosen to preserve the seasonal operation pattern, but also to ensure a smooth computation. All the models were run for 5 years allowing to reach the stabilization of the seasonal recovery efficiency, but also avoiding the interferences that can be generated in the first years of operation of the system.
- Aquifer thermo-hydraulic parameters: a typical sandy aquifer has been simulated with parameters obtained from Beernink et al. 2024 (Table 1).

2.2. Simulations

2.2.1. Sensitivity analysis scenarios

A sensitivity analysis of the three parameters that greatly affect the efficiency of ATES systems was done, keeping the hydraulic conductivity, the porosity and dispersivity constant for all the scenarios. In particular, the chosen parameters are the inter-well distance (*d*), the GW flow velocity (*u*), and the total storage volume (*V*, i.e. the total

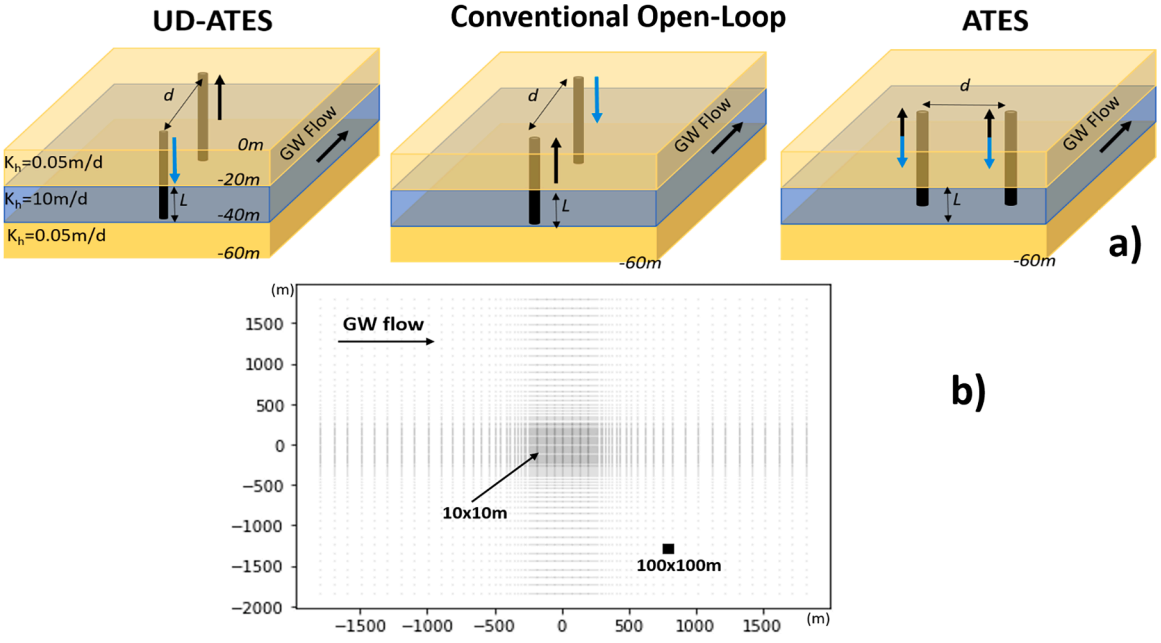

Fig. 2. Schematic representation of: a) the layers in the synthetic model of the three geothermal systems considered, b) the grid size in plan view. (Single column 8 cm width).

Table 1
MODFLOW simulation parameters values (Beernink et al. 2024.).

Parameter	Symbol	Value
Aquifers' horizontal conductivity	K_h	10 m/d
Aquitards' horizontal conductivity	K_h^{aqt}	0.05 m/d
Porosity	n	0.3
Longitudinal dispersivity	α_l	0.5 m
Transversal dispersivity	α_t	0.05 m
Density of solid	ρ_s	2640 Kg/m^3
Density of fluid	ρ_f	1000 Kg/m^3
Bulk density	ρ	2148 Kg/m^3
Solid heat capacity	w_s	710 J/Kg °C
Fluid heat capacity	w_f	4183 J/Kg °C
Thermal conductivity of sand	k_s	2 W/m °C
Thermal conductivity of clay	k_c	1.7 W/m °C
Thermal conductivity of fluid	k_f	0.58 W/m °C
Thermal conductivity of the aquifer	k	1.57 W/m °C
Thermal conductivity of the aquitard	k^{aqt}	1.36 W/m °C
Effective molecular diffusion	α	$1.4{\cdot}10^{-11}$ m^2/day
Thermal distribution coefficient	λ	$1.7{\cdot}10^{-4}$ m^3/Kg

withdrawn or injected GW volume per season).

- The d was varied from 50 m to 350 m, an appropriate distance in an urban context or district scale (with steps of 25 m).
- For each d, different u, varying from 3 m/y up to 1000 m/y, were simulated, similarly to Chae et al. 2020. Smaller steps were used at lower velocities and greater at higher velocities, resulting in the following range: 3–25–30–50–75–100–150–200–250–300–400–500–750–1000 m/y. These values were obtained by changing the hydraulic gradient of the model, since the hydraulic conductivity was kept constant in all the scenarios.
- The different u and d cases were simulated using three different scenarios of V: 100,000, 250,000 and 500,000 m^3/season, being representative of ATES sizes (Bloemendal and Hartog, 2018). The storage volume (V) was distributed over time using a cosine function as shown in Fig. 3.

The wide variability of these parameters is representative of several ATES conditions making this model applicable to all the sites that present any GW flow velocity.

The model configuration started by selecting appropriate values for d. By setting a V value of 250,000 m^3/season and no u. The inter-well distances (d) values from 25 to 500 m, with 25 m steps were used. First, the energy at each time step was obtained (Fig. 4), and secondly all energy values related to one of the two seasons of the fifth year were summed up.

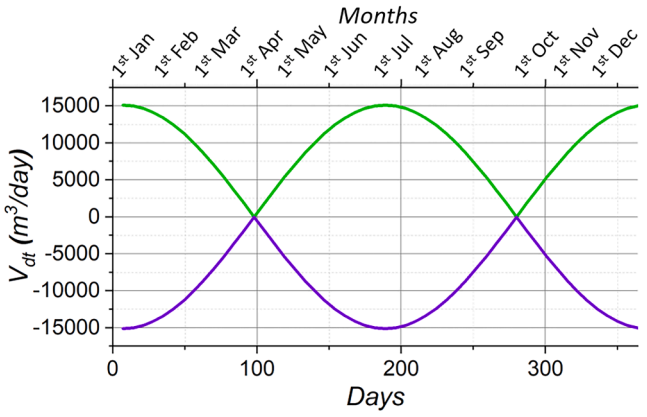

Fig. 3. Cosine distribution of the pumping rate (V_{dt}) for the upstream well (W0, injection) and the downstream well (W1, withdrawal) case, respectively. (Single column 8 cm width).

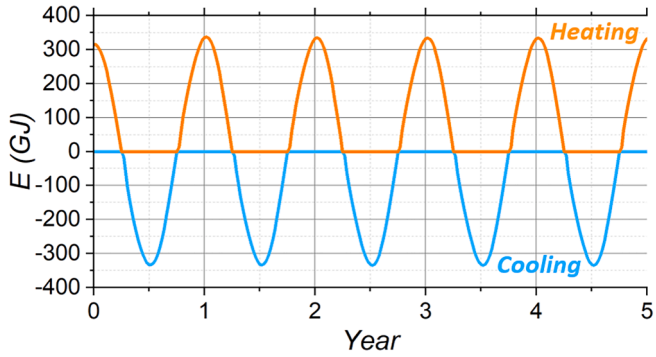

Fig. 4. Winter and summer distribution of energy during five years (example for a d of 150 m). (Single column 8 cm width).

2.2.2. UD-ATES, O-L and traditional ATES scenarios

The hydro-thermal solution results generated for different scenarios (Fig. 2), including the uni-directional ATES (UD-ATES) system, in which the pumping well lies downstream the injection one, the conventional open-loop (O-L) scheme, in which the directions of pumping and injection of the two wells, was reversed, and the traditional ATES configuration, in which the two wells were disposed transversely to the GW flow direction to avoid short circuit flows between the two wells at greater u.

A further difference in the model settings is represented by d (Table 2). In he case of the UD-ATES system, the efficiency for a specific d depends on u and V parameters and was modified accordingly during the sensitivity analysis. Instead, for the traditional ATES and the O-L configurations d was as the minimum value that avoids the short-circuiting effects between the two wells for all u considered, and it is just related to V.

2.3. Assessment framework

2.3.1. Thermal recovery efficiency

The energy extracted from the GW by the system was calculated for each time step by multiplying V by the specific heat capacity of water (c_w), by its density (ρ_w) and by the difference between the extraction (T_{ext}) and injection (T_{inj}) temperatures. Then, the seasonal energy (Eq. (1)) was obtained by integrating over the different seasons:

$$E_{season} = \int_{season\_start}^{season\_end} V_{dt}\cdot(T_{ext} - T_{in})\cdot\rho_w\cdot c_w\cdot dt \quad (1)$$

Where V_{dt} is the volume extracted or injected for each time step, T is the injection/extraction temperature, dt is the time step, c_w is the heat capacity of water.

Within the model the total energy (E_{season}) was retrieved by summing up all the energy values for each time step (7 days), separately for the two different seasons (summer and winter). From this value, the thermal recovery efficiency percentage (η_{th}) (Eq. (2)) was computed by comparison with the maximum potential seasonal energy (E_{max}) that could

Table 2
Variability of the d according to V considered (minimum d to avoid the short circuiting effect).

	Inter-well distance ATES	Inter-well distance O-L	Inter-well distance UD-ATES
100,000 m^3/season	200 m	150 m	Variable according to u
250,000 m^3/season	250 m	200 m	Variable according to u
500,000 m^3/season	300 m	250 m	Variable according to u

be collected in one season for a fixed ΔT of 10 °C. All the results will be evaluated in terms of η_{th}.

Both E_{season} and η_{th} were retrieved starting from the 5th year of simulation, assuming the average annual temperature downstream the injection point to reach stationarity with only seasonal oscillations. This condition has been verified for all the scenarios evaluated in this work.

$$\eta_{th} = \frac{E_{season} \cdot 100}{E_{max}} \ [\%] \tag{2}$$

The results were then assessed based on d as a function of the theoretical thermal radius (R_{th}). The inter-well distance (d) divided by the thermal radius (d/R_{th}) parameter is a dimensionless ratio representing η_{th} for a defined thermal volume (the thermal energy volume stored in the aquifer by the system) in ATES configurations. The R_{th} (Eq. (5)) is also related to the hydraulic radius (R_h) which is defined (Eq. (4)) as the infiltrated volume discretized as a cylinder (Bloemendal and Hartog, 2018), and depends on the injected volume (V_{in}), the porosity (n), the water and aquifer heat capacity (c_w and c_{aq}) and their density (ρ_w and ρ_{aq}) (Eq. (3)).

$$\rho_{aq} \cdot c_{aq} = n \cdot c_w \cdot \rho_w + (1-n) \cdot c_s \cdot \rho_s \tag{3}$$

$$R_h = \sqrt{\frac{V_{in}}{n \cdot \pi \cdot H}} \tag{4}$$

$$R_{th} = \sqrt{\frac{c_w \cdot \rho_w \cdot V_{in}}{c_{aq} \cdot \rho_{aq} \cdot \pi \cdot H}} = \sqrt{\frac{n \cdot c_w \cdot \rho_w}{c_{aq} \cdot \rho_{aq}}} \cdot R_h \approx 0.66 \, R_h \tag{5}$$

Where c_s is the heat capacity of the solid, n is the porosity, and H is the aquifer screen length.

2.3.2. Downstream pollution

The thermal downstream plume was estimated in representative scenarios for the three different geothermal systems considered. The temperature data were collected for each time step in each cell located along the axis of the two wells (for the traditional ATES case the temperature was evaluated on the axis of just one well).

3. Results

3.1. Sensitivity / general analysis

In the following section, the results obtained from the uni-directional ATES (UD-ATES) simulations will be presented.

Fig. 5 shows the recovered thermal energy, expressed as a ratio to the maximum total energy (i.e., η_{th}), for both winter and summer seasons

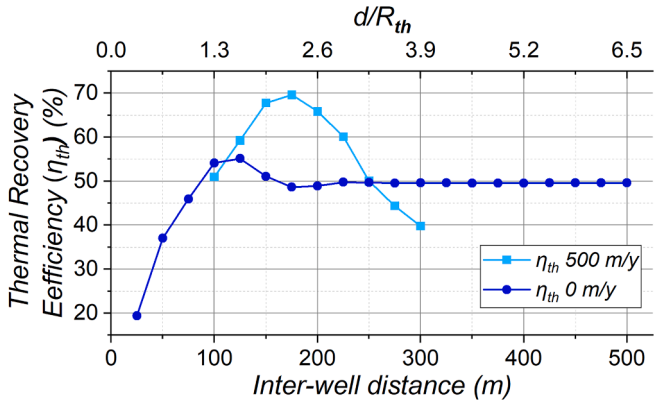

Fig. 5. Thermal recovery efficiency (η_{th}) curves for different d of the uni-directional ATES (UD-ATES) configuration for 0 m/y and 500 m/y of GW flow velocity (u) and a storage volume (V) of 250,000 m^3/season in winter. (Single column 8 cm width).

across various inter-well distances (d) scenarios in the case with no and 500 m/y GW flow velocity (u).

- For the no groundwater flow simulation, when d/R_{th} is low, the thermal recovery efficiency (η_{th}) is low due to the thermal short-circuit occurring between the two wells. As d gradually increases, the energy output also grows due to the less short-circuit effect, peaking at approximately 125 m ($d/R_{th} = 1.62$). This peak can be attributed to the absence of short-circuit flows and the presence of warm/cold water injections from the preceding season. As d further increased, the energy diminishes once again. This drop results from a mismatch between the extraction temperature and the required temperature for heating or cooling the building, until a stable value across greater distances is reached. The second minor peak (at $d/R_{th} = 2.3$) is caused by a favourable alignment between the extraction temperature and the system's required temperature, occurring after two season cycles. Beyond this value of d/R_{th}, the energy experiences a slight decrease, stabilizing at greater values of d/R_{th}. This stabilization occurs due to the absence of any remaining thermal interaction between the two wells. The reason why it stabilizes at 50 % efficiency results from the ambient aquifer temperature which is exactly between the warm and cold temperatures. Hence, η_{th} of 50 % means that ambient groundwater is extracted, while η_{th} lower than 50 % means that groundwater with unfavourable temperature at a specific time is extracted, for example if short-circuiting occurs.
- The results for 500 m/y u scenario show that the peak is shifted to 175 m ($d/R_{th} = 2.27$) since the thermal plume is brought to further distances due to groundwater advection.

Fig. 6 shows η_{th} as a function of d under different u for 100,000 m^3/season (Fig. 6a), 250,000 m^3/season (Fig. 6b), and 500,000 m^3/season (Fig. 6c) V, respectively. All the scenarios were run up to d that is needed to obtain an optimum of efficiency.

The following observations can be done:

- Higher V directly correlates with higher energy recovery. This observation aligns with traditional ATES behaviour, where a larger volume corresponds to improved performance and minimized energy losses.
- Higher u requires a larger d to obtain optimal recovery rates. This is explained by the fact that the plume is transported at further distances throughout each seasonal cycle. On the other hand, at lower d, η_{th} is lower for greater u, since as the velocity increases the short circuit flow between the two wells gets stronger.
- At 100,000 m^3/season V (Fig. 6a), the optimal values remain relatively constant (almost 70 %) for u larger than 400 m/y. However, at 250,000 m^3/season and 500,000 m^3/season V the efficiency exhibits an upward trend (65 % to 75 % in both cases) for higher u, meaning that even higher efficiency may be reached at greater u. This variation according to the different V depends on the fact that the energy is dispersed more rapidly by high u with low V compared to scenarios with greater volumes; for this reason, in the case of 100,000 m^3/season the efficiency does not exceed 70 %.
- Since the maximum efficiency is not close to 100 %, it seems impossible to capture all the thermal energy injected from the upstream well. This is caused by the intermitted warming-up and cooling down of the confining layers. So, every cycle there are relatively large losses to the layers above and below. Also, dispersion and mixing of warm and cold injected water, as well as the mixing with the GW at natural ambient temperature, results in losses.
- All the scenarios located under the 50 % line are representative of a negative short-circuitation effect between the two wells, which results in a strong reduction of η_{th}.
- Furthermore, the optimal distances corresponding to each u in the three V considered showed that are not located at the same value of

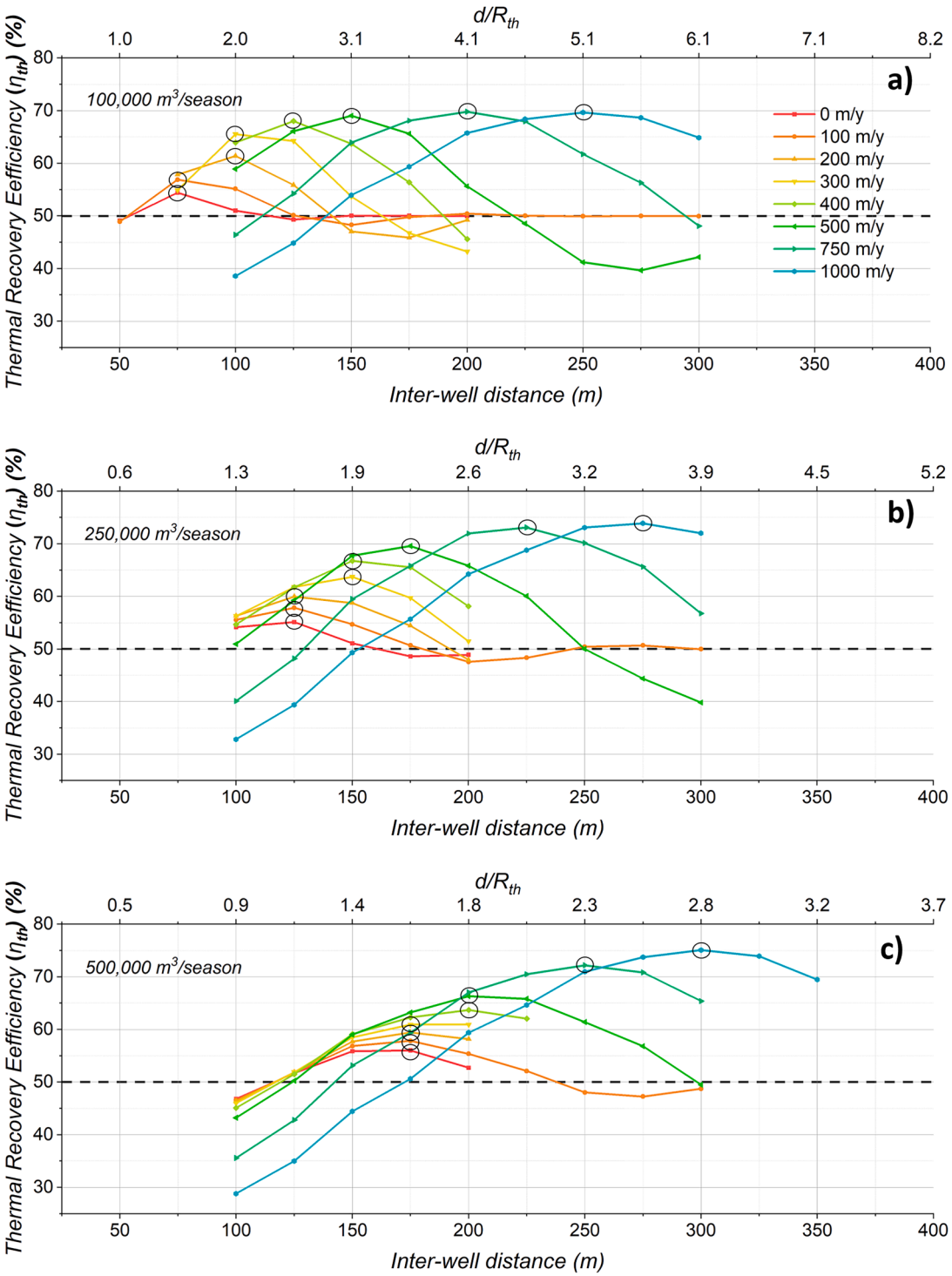

Fig. 6. Thermal recovery efficiency (ηth) as a function of the inter-well distance (d) for different GW flow velocities (u) and different scenarios of storage volumes (V): a) 100,000 m3/season, b) 250,000 m3/season, c) 500,000 m3/season. The upper axes report the ratio between the inter-well distance and the thermal radius (d/Rth) and changes for the three plots since Rth is a function of the storage volume (V). The optimum are depicted with a black circle. The dashed line represents the thermal recovery efficiency (ηth) of a conventional open-loop (O-L) system. (Double column 16 cm width)

d/R_{th}, but they are shifted towards lower values of d/R_{th} and higher values of d for increasing V.

The general concept of recapturing a major part of the injected heat with a downstream well proves to be feasible from these simulation results. Fig. 6. Thermal recovery efficiency (η_{th}) as a function of the inter-well distance (d) for different GW flow velocities (u) and different scenarios of storage volumes (V): a) 100,000 m^3/season, b) 250,000 m^3/season, c) 500,000 m^3/season. The upper axes report the ratio between the inter-well distance and the thermal radius (d/R_{th}) and changes for the three plots since R_{th} is a function of the storage volume (V). The optimum are depicted with a black circle. The dashed line represents the thermal recovery efficiency (η_{th}) of a conventional open-loop (O-L) system. (Double column 16 cm width)

3.2. Comparison amongst ATES and O-L

The model results of the UD-ATES system were compared to the other systems by extracting the optimum η_{th} at the different u and V (Fig. 7). For the traditional ATES and the O-L configuration, the d was varied according to the different V considered, but was kept constant for all the u, since d does not affect η_{th}.

Fig. 7 shows the most efficient system at different u. The O-L system has a constant η_{th} (50 %) in all the scenarios since there are no variations between the extraction and injection temperatures. The η_{th} of both the ATES systems considered, increases at greater V. At small u, the traditional ATES systems perform better, but as the groundwater flow velocities increase the UD-ATES outperforms the traditional ATES system. The threshold value between the UD-ATES and the traditional ATES shifts towards higher u with increasing V, passing from 220 m/y for the smallest V, to 320 m/y for 250,000 m^3/season, up to 400 m/y for the greatest V. This might be explained by the fact that the higher the V, the greater the chances that the traditional ATES extracts back the thermal plume injected in the previous season.

3.3. Downstream thermal plume

The thermal plume generated by the three systems considered was analysed to understand how and at which distance GW users located downstream could be affected.

Fig. 8 show the temperature variation along the flow direction for all the time steps modelled in the fifth year of operation, when the temperatures is stabilized. The lines going from blue to red indicate the increasing number of weeks from the 1st of January to the 31st of December.

For the O-L (Fig. 8a), the temperature (ΔT) is ± 0.5 °C at 80 m from the downstream (injection) well, and ± 0.25 °C at 130 m. For the UD-ATES system (Fig. 8b), the ΔT at the downstream (extraction) well is lower than ± 0.5 °C and decreases to ± 0.25 °C at 15 m from it. For the traditional ATES scenario (Fig. 8c), the distance is calculated downstream the cold well (because the two wells were not disposed on the longitudinal direction of the GW flow, but transversely).

The temperature variation in this case indicates that the ΔT is ± 0.5 °C at 345 m, and decreases to ± 0.25 °C at 375 m. Despite the fact that the injected volume is half compared to the other two cases (since the cold well was considered, only), such a long thermal plume can be explained by the lack of thermal counterbalance during the injection of hot water from the same well.

4. Discussion

The thermal recovery efficiency (η_{th}) of traditional ATES systems is known to be reduced with increasing the GW flow velocity (u). The heat loss due to dispersion is larger at high velocities since the heat is being transported away from the production well, thus reducing the stored heat available for the following season (Bloemendal and Olsthoorn, 2018). In the worst case of a very fast GW flow velocity (> 750 m/y), the efficiency of the ATES systems is reduced to 50 %, equal to a conventional open-loop (O-L) system (Fig. 7). This research demonstrates that, above a certain u, a uni-directional ATES (UD-ATES) configuration can be a worthwhile alternative able to reuse part of the energy extracted or injected into the aquifer during the previous season. In the ideal case of symmetrical heating and cooling demand, the UD-ATES can reach a η_{th} as high as 75 %, much larger than the O-L systems.

The u threshold above which the UD-ATES system outperforms the traditional ATES systems shows a dependence on the storage volume (V), which in turn depends on the annual pumping rate: the larger the V, the higher the u thresholds. This is due to the following reasons: firstly, the larger the V, the more efficient is the traditional ATES systems, where a larger V corresponds to improved performance and minimised energy losses; on the contrary, the UD-ATES, at lower u, suffers from large values of V due to the higher degree of possible interference caused by a large extension of the thermal plume. Meanwhile, greater values of V result in higher values of well discharge, causing higher interference between the wells.

This research also demonstrates that the extent and intensity of the thermal plume is extremely reduced by using a UD-ATES in optimal inter-well distance (d) condition and assuming a symmetrical heating and cooling demand. In the example shown in Fig. 8, the thermal plume length is reduced by approximately one order of magnitude compared to the other systems. This positive effect of UD-ATES on the thermal plume has been observed also for the other u and V values.

The main lack of this study is the assumption of equal heating and cooling loads for summer and winter seasons, in order to maximize η_{th} of the system. However, the actual heating and cooling load of an end-user

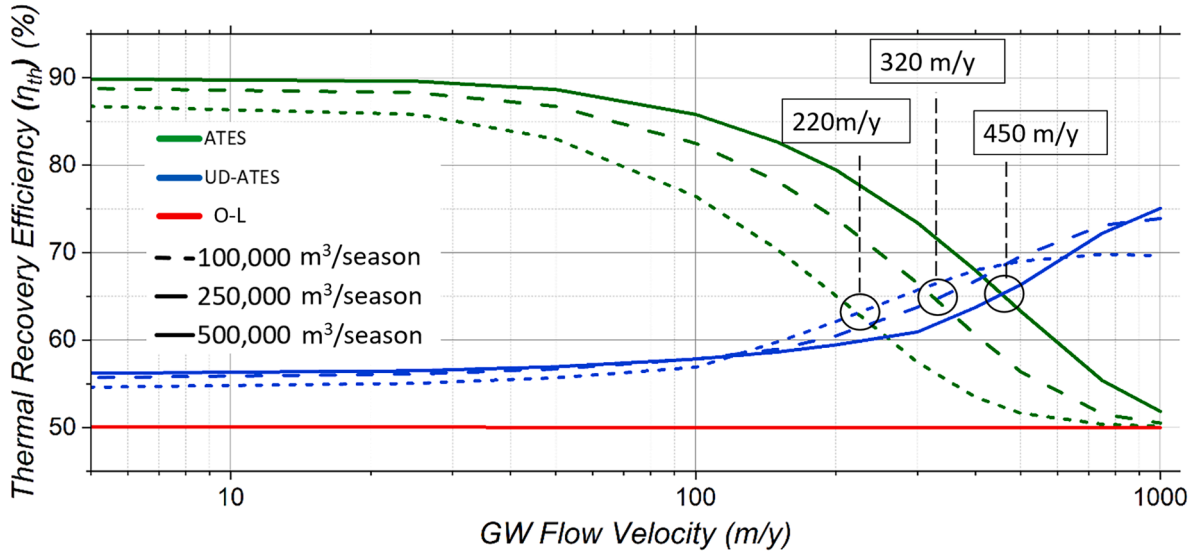

Fig. 7. Comparison of the thermal recovery efficiency (η_{th}) versus the GW flow velocity (u) for the three different geothermal systems considered for the three storage volume (V) scenarios. The efficiency remains constant for the conventional open-loop (O-L) system, but it shows a variation for the other systems with an increase of the GW flow velocity (u). The black circles identify the trade-off values for which the uni-directional (UD-ATES) becomes more convenient than the traditional ATES. (Double column 16 cm width).

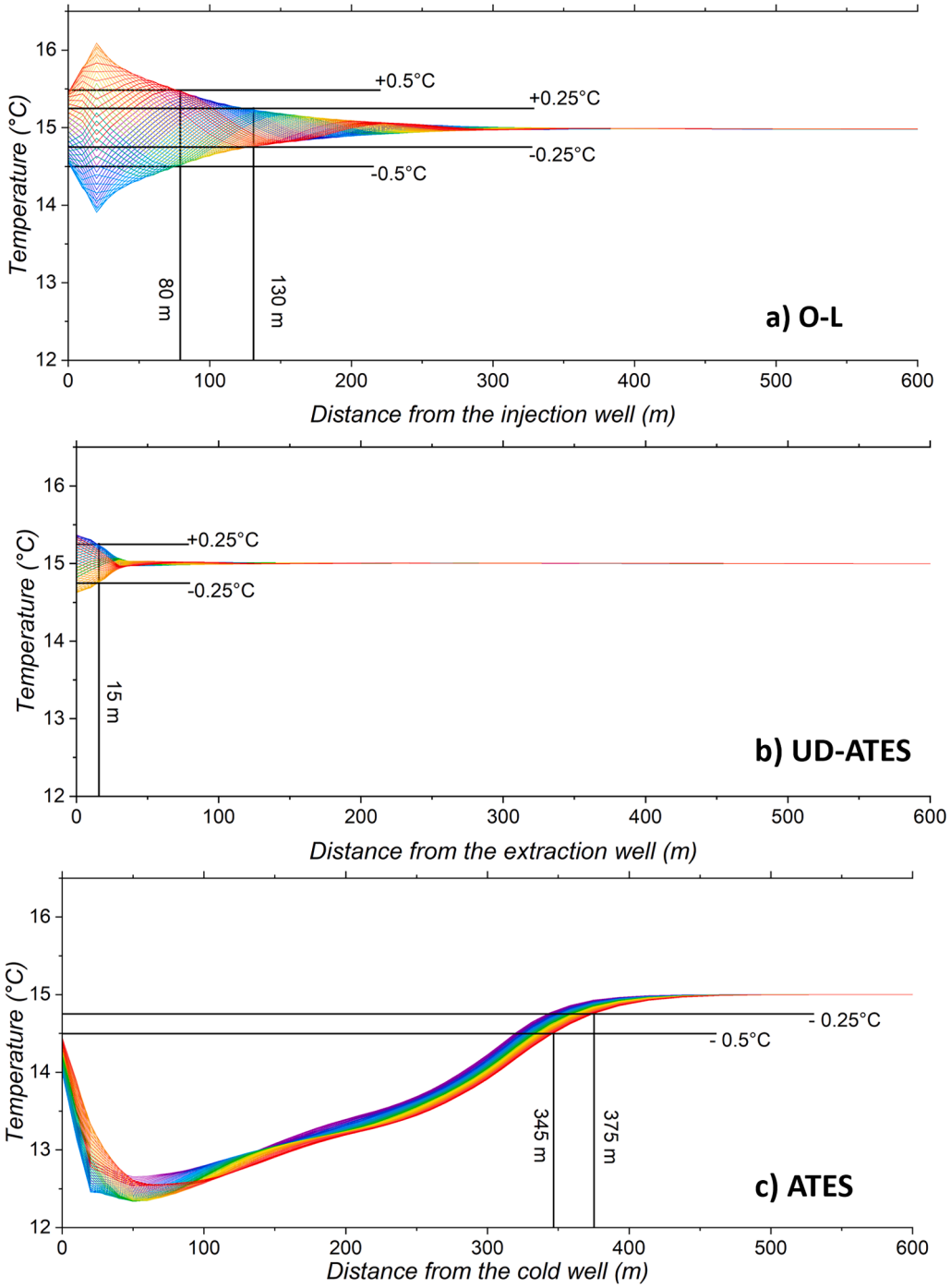

Fig. 8. Temperature variation downstream of the system, during the fifth year of operation, for a GW flow velocity (u) of 300 m/y and a storage volume (V) of 100,000 m^3/season: a) conventional open-loop (O-L) system with inter-well distance (d) of 150 m; b) UD-ATES system with inter-well distance (d) of 110 m; c) traditional ATES system with inter-well distance (d) of 200 m. For the traditional ATES, the temperature downstream is reported for the cold well, and would be specular for the warm well. Each coloured line represent a time step of the analysis (1 week) increasing from blue to red. The distances at the isotherm lines of ±0.5 °C and ± 0.25 °C is marked with black vertical lines. (Double column 16 cm width).

would vary throughout the year, with possible imbalances between the energy demand in summer and winter, resulting in lower η_{th}. Moreover, this imbalance could also affect the long-term sustainability of these systems. Therefore, further study is needed to assess the feasibility of UD-ATES systems compared to other configurations under different energy demand scenarios, e.g., in different climatic zones.

In the following paragraphs will be discussed relevant aspects related to the operability of UD-ATES.

4.1. *Effects of aquifer thickens and thermal dispersivity*

The aquifer thickness (H) and the mechanical dispersivity (α_l) were not formally included in the sensitivity analysis. However, the effect of the variation of these two parameters on d and η_{th} was analysed for a specific V (100,000 m^3/season) and for moderately low and high u (100 and 500 m/y).

Different scenarios with 10–20–30–40–50 m thick aquifers were tested. Generally, it was observed that, independent of u, the optimal

d decreases with greater values of H (Fig. 9a), while minimal variations in η_{th} are observed (Fig. 9b). This could be related to the different horizontal/vertical shape ratio of the thermal plume, e.g., expressed by the thermal radius of Eq. (5). Additionally, there is slight evidence that for different u, there is an optimal aquifer thickness giving a maximal value of η_{th} (Fig. 9b).

The longitudinal dispersivity, α_l, tested in the different scenarios run was 0.1–0.5–1–5–10–50 m, whereas the transversal dispersivity was always set at one order of magnitude less than the longitudinal one. Different values of dispersivity cause variations in the extent and the temperature field inside the thermal plume. This leads to losses in η_{th} for higher values of α_l, with a stronger effect for greater flow velocity (Fig. 9d). Due to the thinning of the temperature profile along with the thermal plume, for higher values of α_l, d tends to a common value for different values of u (Fig. 9c).

4.2. Effects of natural variability of groundwater flow velocity and direction

To configure and build UD-ATES systems it is important to have a thorough understanding of the GW flow direction and *u* in the aquifer used as storage. Once a UD-ATES is designed, and the *d* fixed, a natural variation of *u* or direction can affect the performance of the system. The effect of GW flow *u* and direction on η_{th} of UD-ATES was quantified by modelling different scenarios considering a fixed *V* of 100,000 m^3/season, a *d* of 110 m, and a *u* of 300 m/y. By reducing the *u* by 5 %, 10 % and 15 %, the η_{th} dropped by 0.7 %, 1.5 % and 2.5 % respectively. At the same time, modifying the GW flow direction by 5°, 10° and 15° from the longitudinal direction of the two wells in respect to the GW flow direction reduces the η_{th} by 0.2 %, 1.0 % and 2.6 %, respectively.

These scenarios demonstrate that a good knowledge of the GW flow direction and *u* is imperative to establish the best position and *d* of the doublets, which allows to obtain the maximal η_{th} from the system.

The best way to estimate the GW flow *u* and direction is to perform direct measurements through a long-term monitoring, to characterise their variations over time. In this way, it would be possible to test the model within the entire range of variability of these parameters and to evaluate how much η_{th} could change in specific periods, reducing the operation risks.

4.3. Cost comparison

Furthermore, in a dense urban setting, such as metropolitan cities, several geometric constraints may also hamper the installation of wells at the optimal required spacing and orientation to obtain the maximum η_{th} from the system. It is important to run several numerical models to evaluate the most suitable *d* and direction according to the geometrical constraints, in order to establish which system could be the most efficient. The need for a detailed characterization of the aquifer, which is mandatory to optimize the efficiency of the system, can lead to higher capital expenditure (CAPEX) compared to O-L and traditional ATES. However, the paper shows that an optimal configuration of the UD-ATES system in high *u* velocity aquifers can be 13 to 25 % more efficient compared to O-L system. This higher efficiency translates into a reduction in the energy required to extract and inject water, resulting in lower operating costs (OPEX) for the system. In the long term, this should compensate for the higher CAPEX. Furthermore, greater efficiency results in lower storage volume. In this way, it might be possible to decrease the number of wells needed for system operation, reducing the relative cost. In particular, the UD-ATES system seems promising in regions with high u, such as in the Po plain of northern Italy. More generally, regions with high aquifer productivity (e.g. Sprenger et al. 2017) are all suitable for ATES systems (either traditional or uni-directional). In any case, it is important to assess the local hydraulic gradient to decide which system is best.

4.4. National regulation

Traditional ATES systems are installed worldwide (Sweden, Belgium, Denmark, and the USA), but more than 90 % of them are operating in the Netherlands (Hoekstra et al., 2020). This is because the aquifers in this country are characterized by low GW flow velocity due to the strong

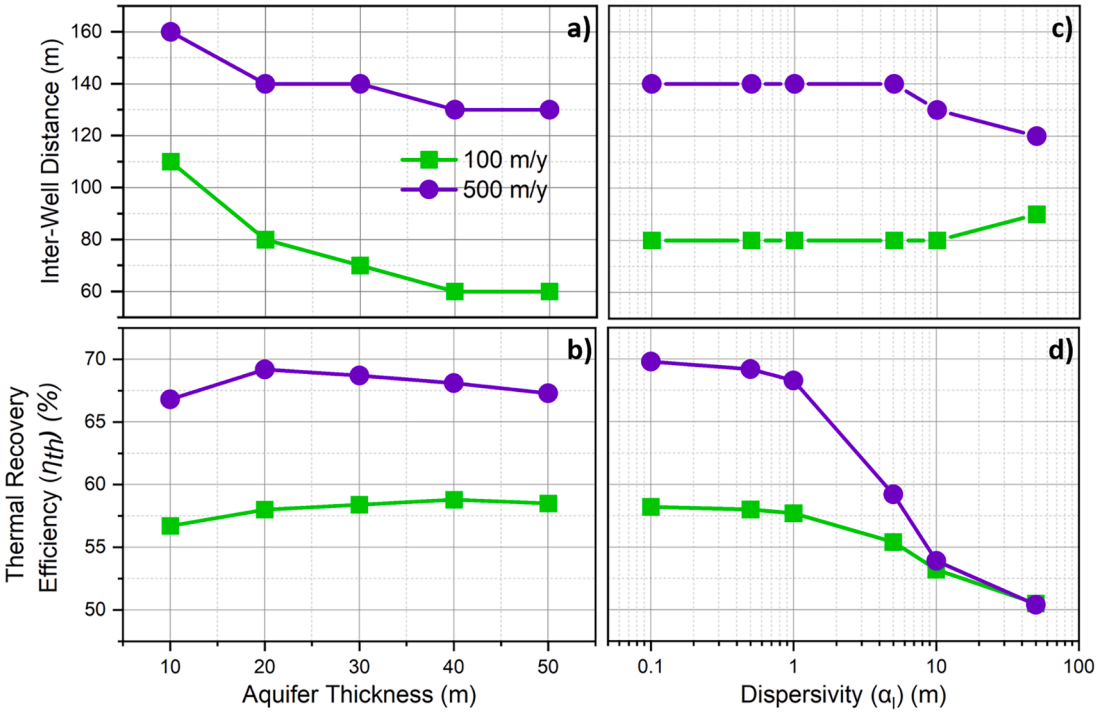

Fig. 9. a-b) aquifer thickness (H) vs inter-well distance (d) and thermal recovery efficiency (η_{th}), respectively. c-d) longitudinal dispersivity (α_l) vs inter-well distance (d) and thermal recovery efficiency (η_{th}), respectively. (Double column 16 cm width).

presence of fine sandy layers and gradients close to 0 %. In many other locations, except for these countries, there are not yet any regulations for ATES systems, because O-L configurations are more popular and widely used. In the most populated Italian Region (Lombardy), for instance, there is currently no legislation to regulate the adoption of ATES systems. In this region, the regulation (Regione Lombardia, 2017) states that the temperature difference between the extraction and injection wells must be lower than 5 °C, not allowing the operation of a well doublet with an ATES configuration. Therefore, to promote this technology we propose to consider a maximal threshold value of temperature difference with respect to the natural ambient temperature of the GW.

5. Conclusions

This study investigated the behaviour of uni-directional ATES (UD-ATES) systems, a concept of aquifer thermal energy storage (ATES) that uses groundwater flow to store and recover thermal energy. The study performed a sensitivity analysis of the UD-ATES system for different conditions of inter-well distance (d), GW flow velocity (u), and storage volume (V). The study also compared the UD-ATES system with other ATES/open-loop systems, such as traditional ATES and conventional open-loop (O-L) systems, in terms of thermal recovery efficiency (η_{th}), temperature variation, and downstream thermal plume. The study demonstrates that the UD-ATES system is feasible, especially for high u, as it can retrieve a major part of the thermal energy stored in the aquifer by a downstream well, despite heat losses due to groundwater flow. Recovery by a downstream well is controlled by choosing an appropriate d, depending on the V and the u.

The UD-ATES system can increase the efficiency of the thermal energy storage at high u, contrary to O-L systems which is not capable to store heat. The UD-ATES system can be from 16 to 25 % more efficient for u greater than 500 m/y, while traditional ATES can be from 18 to 40 % more efficient for u lower than 400 m/y.

Examining the case of 100,000 m^3/season at u lower than 220 m/y, the traditional ATES system is more efficient, while for greater values, the UD-ATES is more convenient. This threshold value shifts to greater u according to which V is considered.

Moreover, the UD-ATES system can reduce the temperature variation and the downstream thermal plume, compared to O-L systems. The thermal plume of an O-L system can be up to 6 times longer than the one generated by a UD-ATES configuration under the same conditions.

Hence, the UD-ATES system can achieve two goals simultaneously: increasing the efficiency of the thermal energy storage wells and reducing the thermal pollution downstream, to avoid undesirable interactions between different systems located upstream and downstream.

The limitations and challenges of a UD-ATES system are the risk of short-circuit flow, which could reduce the η_{th} below 50 %, and the effect of uncertainties and variations in well placement options, groundwater flow direction and u, and heating and cooling load. The study contributes to the development of a new ATES concept that can improve the performance and sustainability of O-L systems, by providing insights and guidelines for the design and operation of UD-ATES systems. Future research should focus on validating the UD-ATES model with field data and exploring the potential of UD-ATES systems for different applications and scenarios.

CRediT authorship contribution statement

Valerio Silvestri: Writing – original draft, Visualization, Software, Methodology, Investigation, Formal analysis, Data curation, Conceptualization. **Giovanni Crosta:** Writing – review & editing, Supervision, Funding acquisition, Conceptualization. **Alberto Previati:** Writing – review & editing, Visualization, Software, Data curation. **Paolo Frattini:** Writing – review & editing, Supervision, Funding acquisition, Conceptualization. **Martin Bloemendal:** Writing – review & editing, Supervision, Funding acquisition, Conceptualization.

Declaration of competing interest

The authors declare that they have no known competing financial interests or personal relationships that could have appeared to influence the work reported in this paper.

Data availability

The data are public, but the code used for the numerical model is confidential.

Acknowledgements

This work was realized thanks to the PON funding related to the project named “BICMIB - Blue-green infrastructures for the City of Milano in Bicocca”, which funded also the abroad period at TU Delft with the supervision of Martin Bloemendal.

A special thanks goes to Stijn Beernink who helped in modifying flopys’ code to the needs of this study.

Supplementary materials

Supplementary material associated with this article can be found, in the online version, at doi:10.1016/j.geothermics.2024.103152.

References

Bakker, M., Post, V., Langevin, C.D., Hughes, J.D., White, J.T., Starn, J.J., Fienen, M.N., 2016. Scripting MODFLOW model development using Python and FloPy. Groundwater 54 (5), 733–739.

Banks, D., 2009. An introduction to ‘thermogeology’ and the exploitation of ground source heat. Q. J. Eng. Geol. Hydrogeol.

Beernink, S., Hartog, N., Vardon, P.J., Bloemendal, M., 2024. Heat losses in ATES systems: the impact of processes, storage geometry and temperature. Geothermics 117, 102889.

Bloemendal, M., Hartog, N., 2018. Analysis of the impact of storage conditions on the thermal recovery efficiency of low-temperature ATES systems. Geothermics 71, 306–319.

Bloemendal, M., Jaxa-Rozen, M., Olsthoorn, T., 2018. Methods for planning of ATES systems. Appl. Energy 216, 534–557.

Bloemendal, M., Olsthoorn, T., van de Ven, F., 2015. Combining climatic and geo-hydrological preconditions as a method to determine world potential for aquifer thermal energy storage. Sci. Total Environ. 538, 621–633.

Bloemendal, M., Olsthoorn, T., 2018. ATES systems in aquifers with high ambient groundwater flow velocity. Geothermics 75, 81–92.

Chae, H., Nagano, K., Sakata, Y., Katsura, T., Kondo, T., 2020. Estimation of fast groundwater flow velocity from thermal response test results. Energy Build. 206.

Fleuchaus, P., Schüppler, S., Godschalk, B., Bakema, G., Blum, P., 2020. Performance analysis of aquifer thermal energy storage (ATES). Renew. Energy 146, 1536–1548.

Harbaugh, A.W., Banta, E.R., Hill, M.C., McDonald, M.G. 2000. Modflow-2000, the U.S. Geological survey modular ground-water model-user guide to modularization concepts and the ground-water flow process.

Hoekstra, N., Pellegrini, M., Bloemendal, M., Spaak, G., Gallego, A.A., Comins, J.R., Grotenhuis, T., Picone, S., Murrell, A.J., Steeman, H.J., Verrone, A., Doornenbal, P., Christophersen, M., Bennedsen, L., Henssen, M., Moinier, S., Saccani, C., 2020. Increasing market opportunities for renewable energy technologies with innovations in aquifer thermal energy storage. Sci. Total Environ. 709, 136142.

Lee, K.S., 2014. Effects of regional groundwater flow on the performance of an aquifer thermal energy storage system under continuous operation. Hydrogeol. J. 1 (22), 251–262.

Regione Lombardia (2017), Decreto Giunta Regionale, DGR/6293/17, definition of the implementation methods and content of the preventive studies required by LR 38/2015, for the purpose of authorising the discharge of groundwater extracted for heat pump heat exchange into the aquifer.

Rostampour, V., Jaxa-Rozen, M., Bloemendal, M., Kwakkel, J., Keviczky, T., 2019. Aquifer Thermal Energy Storage (ATES) smart grids: large-scale seasonal energy storage as a distributed energy management solution. Appl. Energy 242, 624–639.

Sprenger, C., Hartog, N., Hernández, M., Vilanova, E., Grützmacher, G., Scheibler, F., Hannappel, S., 2017. Inventory of managed aquifer recharge sites in Europe:

historical development, current situation and perspectives. Hydrogeol. J. 25 (6), 1909.
Stemmle, R., Lee, H., Blum, P., Menberg, K., 2023. City-scale heating and cooling with Aquifer Thermal Energy Storage (ATES). Hydrology and Earth System Sciences Discussions 2023, pp. 1–27.
Zheng, C., Wang, P.P., 1999. MT3DMS: A Modular Three-Dimensional Multispecies Transport Model for Simulation of Advection, Dispersion, and Chemical Reactions of Contaminants in Groundwater Systems; Documentation and User's Guide.

Website References

European Council, 2021. Fit for 55. https://www.consilium.europa.eu/en/policies/green-deal/fit-for-55-the-eu-plan-for-a-green-transition/.
IRENA, 2023. Power to Heat and Cooling: Status. https://www.irena.org/Innovation-landscape-for-smart-electrification/Power-to-heat-and-cooling/Status.
ISPRA, 2020. Flussi di Energia e Domestic Energy Footprint. https://indicatoriambientali.isprambiente.it/sys_ind/1327.